Nutrition 67–68 (2019) 110517

Contents lists available at ScienceDirect

Nutrition

journal homepage: www.nutritionjrnl.com

Basic nutritional investigation

Protection in a model of liver injury is parallel to energy mobilization capacity under distinct nutritional status

Bérengère Papegay M.D. [a], Vincent Nuyens B.Sc. [a], Adelin Albert Ph.D. [b], Mustapha Cherkaoui-Malki Ph.D. [c], Oberdan Leo Ph.D. [d], Véronique Kruys Ph.D. [d], Jean G. Boogaerts M.D., Ph.D. [a], Joseph Vamecq M.D., Ph.D. [e,*]

[a] Division of Experimental Medicine, University Hospital Center, Charleroi, Belgium
[b] Department of Biostatistics, University Hospital of Liège, Liège, Belgium
[c] Université de Bourgogne-Franche Comté, Laboratoire BioPeroxIL (Biochimie du Peroxysome, Inflammation et Métabolisme Lipidique) Dijon, France
[d] Immunobiology and Molecular Biology of the Gene, Department of Molecular Biology, Free University of Brussels (ULB), Gosselies, Belgium
[e] Inserm, Biochemistry and Molecular Biology Laboratory, North France University Lille, France

ARTICLE INFO

Article History:
Received 24 December 2018
Received in revised form 6 March 2019
Accepted 8 May 2019

Keywords:
Nutritional status
Energy mobilization
Autophagy
Liver injury model
LC3II
Organ protection
Liver cytolysis

ABSTRACT

Objective: Dietary and energetic restrictions are endowed with protection against experimental injuries. However, a drop in cell energetic status under a critical threshold may prevent protection, as previously observed for livers isolated from rat donors undergoing 18-h fasting versus feeding. The aim of this study was to further explore, in the latter model, links between nutritional status, energy availability, and protection through lengthening of rat fasting to 24 h and withdrawal of energy sources from perfusions.
Methods: Energy-free perfused ex vivo livers from fed, 18-h–fasted, and 24-h–fasted rats were studied during 135 min for cytolysis (potassium, aspartate aminotransferase, alanine aminotransferase, and lactate dehydrogenase releases in perfusates), cell deaths (activated caspase-3 [apoptosis], LC3 II/actin and p62/actin ratios [autophagy]), glycogen stores, glucose, and lactate production.
Results: Cytolysis was significantly increased by 18-h and 24-h fasting versus feeding but unexpectedly the increase was less for 24-h fasting than it was for 18-h fasting. Apoptotic marker caspase 3 significantly increased under fed and 18-h fasting but not 24-h fasting conditions. Autophagic marker LC3 II/actin significantly increased during perfusion in the 24-h fasted group but neither fed nor 18-h fasted groups. Autophagic induction also was supported by a drop in the p62/actin ratio. Under perfusion with 3-methyladenine, a standard autophagy inhibitor, protection and enhanced autophagy provided by 24-h but not 18-h fasting were lost without affecting apoptosis.
Conclusions: Liver protections are obviously influenced by nutritional status in a way that is parallel to hepatic energy mobilization capacities (glycogen plus autophagy) with a decreased order of protection: Fed >24-h fasted >18-h fasted >24-h fasted + 3-methyladenine livers. By showing that autophagy induction limits starvation-induced cytolysis, the present work supports the emerging view that autophagy inducers might improve health benefits of diet restriction.

Introduction

The protective properties of dietary and energetic restrictions in health, aging, and disease models assessed through experimental injuries have been previously considered, along with the counterbalanced view that a reduction in cell energy availability under a critical threshold may prevent protection [1]. This latter aspect was inferred from studies on livers isolated from rat donors undergoing 18-h fasting versus feeding and showing an exacerbation by 18-h fasting of ex vivo liver cytolysis [1]. In this respect, necrosis, apoptosis, and autophagy represent cell deaths that are accidental, programmed, and programmed with optional survival, respectively [2,3]. Extrinsic and intrinsic apoptosis recruit plasma membrane (death-inducing signaling complex [DISK]) and soluble apoptosomes, respectively [4], to trigger auto-activation of initiating caspases, which in turn activate executioner caspases for protein cleavage and changes observed during apoptosis [5]. Autophagy involves autophagosomes (encompassing intracytoplasmic components and organelles), which fuse with lysosomes for content degradation; it may lead to cell death or under nutrient deprivation [6] supply energy compatible with cell survival [7].

Declaration of interests: The authors declare that they have no known competing financial interests or personal relationships that could have appeared to influence the work reported in this paper.

* Corresponding author: Tel.: +33 320 44 5694; Fax: +33 320 44 5693.
E-mail address: Joseph.vamecq@inserm.fr (J. Vamecq).

https://doi.org/10.1016/j.nut.2019.05.009
0899-9007/

As mentioned previously, exacerbation of cytolysis and a reduction below a critical energy threshold were previously documented in ex vivo perfused livers originating from 18-h fasted versus fed rats [1,8]. The primary goal of carrying out the present study was to work under energy-deprived perfusion and perform a lengthening of starvation period that precedes liver isolation. The latter was done to provide an additional exacerbation of fasting-driven susceptibility to liver cytolysis previously reported in our liver model [1]. The reason for this strategy was to amplify and hence better characterize key determinants responsible for the difference observed in cytolysis between fed and starved states. Unexpectedly, increasing the starvation period reduced the exacerbation of cytolysis. This has led, secondarily, to consider mechanisms that might protect against fasting-driven cytolysis. In fact, assessing cell death pathways (apoptosis and autophagy) along with energetic stores in various nutritional states leads to a better understanding of the two issues in our liver model: differences in cytolyses between fed and starved states and mechanisms that might protect against fasting-driven exacerbation of cytolysis. Apoptosis is monitored by changes in activated caspase-3 (extrinsic and intrinsic apoptosis) [9]. Autophagy is assessed by increase in the LC3 II/actin ratio (and decrease in the p62/actin ratio) [10–12] and is modulated by 3-methyladenine (3-MA), a specific inhibitor of autophagy [13].

Materials and methods

Ethics

The Animal Care Use and Review Committee of the Belgian Free University of Brussels (CEBEA-IBMM-2014-39) authorized all animal studies.

Animals

Female Wistar rats purchased from Charles River Laboratories (Saint Germain Nuelles, France) with a body weight of 200 g were acclimatized for ≥5 d to the room temperature of 24°C to 26°C with a 12/12-h light/dark cycle. Standard laboratory chow and water were provided ad libidum. Animals were randomly allocated to fed (n = 15) and fasted groups (n ≥ 10 in each group), 18-h (n = 15) and 24-h (n = 10) fasted groups keeping free access to tap water, with food withdrawn 18 and 24 h before liver isolation, respectively. Challenge of 24-h fasted group by 3-MA (n = 10) was done by compound inclusion in perfusion of removed livers, avoiding animal exposure to in vivo compound side effects.

Solutions and chemicals for liver perfusions

Albumin-free Hank's Balanced Salt Solution (HBSS) included 0.4 g/L KCl, 0.06 g/L KH_2PO_4, 0.35 g/L $NaHCO_3$, 0.048 g/L Na_2HPO_4, and 0.14 g/L $CaCl_2$. HEPES 2.38 g/L were added. All chemicals were obtained from Sigma (Bornem, Belgium). The solution was saturated with 100% oxygen (0.5 L/min), pH adjusted to 7.35 ± 0.05 using NaOH 1.0 M and supplemented with NaCl to achieve 300 mOsm. In part of experiments with livers from 24-h fasted rats, HBSS mixture contained 5 mM 3-MA (Sigma-Aldrich, Bornem, Belgium). The 24-h fasting + 3-MA and 24-h fasting groups were perfused by HBSS mixtures supplemented and not with 5 mM 3-MA, respectively.

Hepatectomy and ex vivo liver perfusion

The procedure for liver removal and perfusion was described extensively elsewhere [8,14]. Briefly, animals were anesthetized with pentobarbital sodium (Nembutal, Ceva, Libourne, France) intraperitoneally (50 mg/kg), the abdomen was opened, and heparin (5000 IU/kg) was administered via the inferior vena cava. The portal vein was cannulated with a 22-gauge catheter, secured in place, and immediately perfused with the adequate solution. The liver was removed under continuous perfusion and transferred to the closed system ex vivo arrangement. The system (circuit volume of 125 mL) was maintained at 37°C. The perfusate (i.e., enriched HBSS solution supplemented or not with 5 mM 3-MA) passed sequentially through a peristaltic pump (Ismatec Reglo, Fisher Bioblock Scientific, Tournai, Belgium) at a flow rate of 5 mL/min to obtain a perfusion pressure around 12 cm water through the portal vein.

General protocol for liver biopsies and perfusate sampling

The protocol included 135-min perfusion of livers with respective solutions. Perfusate samples were collected every 15 min and thin liver biopsies were done at 0 and 135 min with instantaneous immersion in either liquid nitrogen with storage at −80°C before determination of LC3 II and p62 autophagy marker or in 10% formalin before postponed embedding in paraffin before immunohistochemistry of caspase-3 (apoptosis) and periodic acid Schiff (PAS) staining (glycogen). For apoptosis, livers embedded in paraffin were cut by a microtome with deposition of slices on optic microscopic glasses. The latter were kept at room temperature for 24 h before deparaffinization and processing for caspase-3 immunostaining mentioned in the section on apoptosis and caspase-3.

For PAS staining, liver slice deparaffinizations and staining with periodic acid were performed by a Tissue Tek Prisma apparatus (Sakura, Europe). PAS-stained slices were processed for determination of glycogen contents in hepatocytes at two time points (0 and 135 min), using the Image J software (National Institutes of Health [NIH], Bethesda, MD, USA) [14]. Five fields per PAS-stained slide were analyzed by a video microscope (Leitz Dialux 20 ES, Leitz, Wetzlar, Germany) equipped with a × 40 objective and combined with a personal computer [8]. Generated pictures were captured onto the hard drive of the workstation computer. Thereafter, captured images were opened in Image J program (NIH) for evaluating indices of positivity on PAS slides. We selected the threshold of glycogen content of all cells (X value) and we referred it to the surface of all cells (Y value). From these area data, the glycogen index for the image was calculated and expressed as a percentage (X/Y).

Perfusate markers and liver biopsy glycogen contents

Aspartate aminotransferase (AST, IU/L), alanine aminotransferase (ALT, IU/L), lactate dehydrogenase (LDH, IU/L), glucose (mg/dL), lactate (mmol/L), and potassium (mEq/L) were assayed in perfusate samples on an Architect plus CI4100 (Abbott Diagnostics, Chicago, IL, USA). Glycogen contents were determined as mentioned previously.

Apoptosis and caspase-3

Apoptosis was evaluated in a blinded fashion using light microscopy after in situ immunostaining. Deparaffinized liver sections were pretreated: hot citrate buffer pH 6.0, inhibition of endoperoxydases with methanol/hydrogen peroxide–blocking cross-reaction (Immunologic, Duiven, The Netherlands), and inhibition of endo-biotin (Vector, Burlingame, CA, USA). Slides were incubated at 4°C overnight using a specific primary antibody for activated cleaved caspase-3 (Caspase-3 ASP 175, Cell Signaling Technology, Danvers, MA, USA) at a 1:100 dilution. Signal amplification was performed with incubation of the complex Ultrasens Streptavidin Peroxidase RTU (Immunologic, Duiven, The Netherlands). Revelation was done with diaminobenzidine (Biogenex, Fremont, CA, USA). Slides were counterstained with Toluidine blue. Apoptosis activity was expressed as the percentage of apoptotic cells (reported on number of hepatocytes) in selected regions. Five fields of each stained slide were analyzed. Apoptosis counting was performed with the image J software using a selection of cells immunolabeled for activated caspase-3, a determination of total and labeled cells by the image J cell counter, and a subsequent calculation of labeled to total liver cell ratios.

Autophagy, LC3 II, and p62 to actin ratios

LC3 II and actin were assayed by Western blot. After defrosting from −80°C, liver biopsies were weighed and protein concentrations determined to load Western blot gels with similar amounts of proteins. Biopsy was grinded in a microvial containing a protease inhibitor (mini EDTA-free pellets, Roche, Basel, Switzerland), phosphate-buffered saline, and Lysing Matrix D Bulk on a Fast Prep Instrument (MP Biomedicals, Santa Ana, CA, USA). It was diluted in a Laemmli buffer (Tris 60 mM pH 6.8, 10% glycerol, 0.01% bromophenol blue, 5% β-mercaptoethanol, 2% sodium dodecyl sulfate [SDS]) to disrupt disulfide bonds and negatively charge proteins for size-based separation. We added 1 μL Benzonase (Novagen, EMD Millipore Corporation, Temecula, CA, USA). Samples were heated to denature proteins, loaded in wells in 10% polyacrylamide/bisacrylamide gel (PAGEr EX Gels, Lonza, Rockland, ME, USA) in a ProSieve Ex Running Buffer (Lonza) and submitted to 100 volts for 10 min and 150 volts until complete migration of the markers. Gel was transferred onto membrane using a transfer buffer (25 mM Tris pH 7.6, 192 mM Glycine, 0.03% SDS, 20% methanol) under 100 volts during 2 h at 4°C, checking complete transfer of proteins with Red Ponceau. Membrane was incubated for 1 h in Tris-buffered saline Tween 20 + 5% milk at room temperature before incubation with a primary antibody LC3 B (#2775, rabbit 1: 1000, Cell Signaling Technology) at 4°C overnight. For LC3 II detection, a horseradish peroxidase-coupled secondary antibody (Promega, Madison, WI, USA) was added 40 min at room temperature and stirred for chemiluminescence with reading after disclosure with substrate of enzyme Western lighting plus electrochemiluminescence (Perkin-Elmer, Waltham, MA, USA). For p62 detection, donkey antirabbit secondary antibody coupled to IRdye 680 (Li-Cor,

Lincoln, NE, USA, 1:15000) was added for 1 h at room temperature with stirring for reading on the Odyssey FC (Li Cor) on the channel 700. Actin levels were measured by chemiluminescence using a mouse antiactin (1:50,000, monoclonal Anti-β-Actin-Peroxidase antibody, Sigma-Aldrich, St Louis, MO, USA). LC3 II-to-actin and p62-to-actin ratios were calculated from respective protein determinations.

Statistical analysis

Results of liver solutes were expressed as mean and SD and similarly for enzymes after a log-transform to normalize their distribution and homogenize their variances. The effect of experimental conditions on their evolution during the 135-min perfusion was tested by Zerbe's method for growth and response curves, which allows comparing groups at each time point and over any time interval. For glycogen content and ratios, data were displayed as boxplots (median and interquartile range). Changes between T_0 and T_{135} were assessed by the Wilcoxon signed rank test, whereas the Kruskal–Wallis test was used for between-group comparisons. Calculations and graphs were done using SAS version 9.4 and R version 3.2.2 statistical packages (SAS Institutes, Cary, NC, USA). Significance was considered at the 5% critical level ($P < 0.05$).

Results

Perfusate marker liver solutes

Figure 1A illustrates time-dependent changes in perfusate solutes in the four experimental groups. Perfusate glucose concentrations in the fed group were systematically higher ($P < 0.0001$) than in the 18-h, 24-h, and 24-h + 3-MA fasted groups and likewise for lactate values. Glucose and lactate concentrations were also significantly lower ($P < 0.0001$) in the 18-h fasted group than in the two 24-h fasted groups. Potassium concentrations in the fed group were significantly lower than in the 18-h fasted ($P < 0.05$) and 24-h fasted + 3-MA groups ($P < 0.001$) after 90 and 60 min of perfusion, respectively. They also were lower in the 24-h fasted group than in the 24-h fasted + 3-MA group after 75 min ($P < 0.01$).

Perfusate marker liver enzymes

Liver enzyme releases in perfusate samples are illustrated in Figure 1B. Values statistically significant are depicted for each group at 135 min. However, the kinetics of the considered enzyme release showed significant differences from 60 to 120 min over the perfusion period. Basically, enzyme levels in 24-h fasted group were observed between those of fed and 18-h starved groups; however, the highest enzyme activities were recorded in 24-h fasted + 3-MA group. AST values were significantly lower in the fed group than in the other three groups ($P < 0.001$). AST in the 24-h fasted group was significantly lower than in the 24-h fasted + 3-MA ($P < 0.001$) and 18-h fasted ($P < 0.05$) groups. After 90 min of perfusion, AST curves were highest in the 24-h fasted + 3-MA group, lowest in the fed group and intermediate in the other two groups, values in 18-h fasted being higher than in 24-h fasted

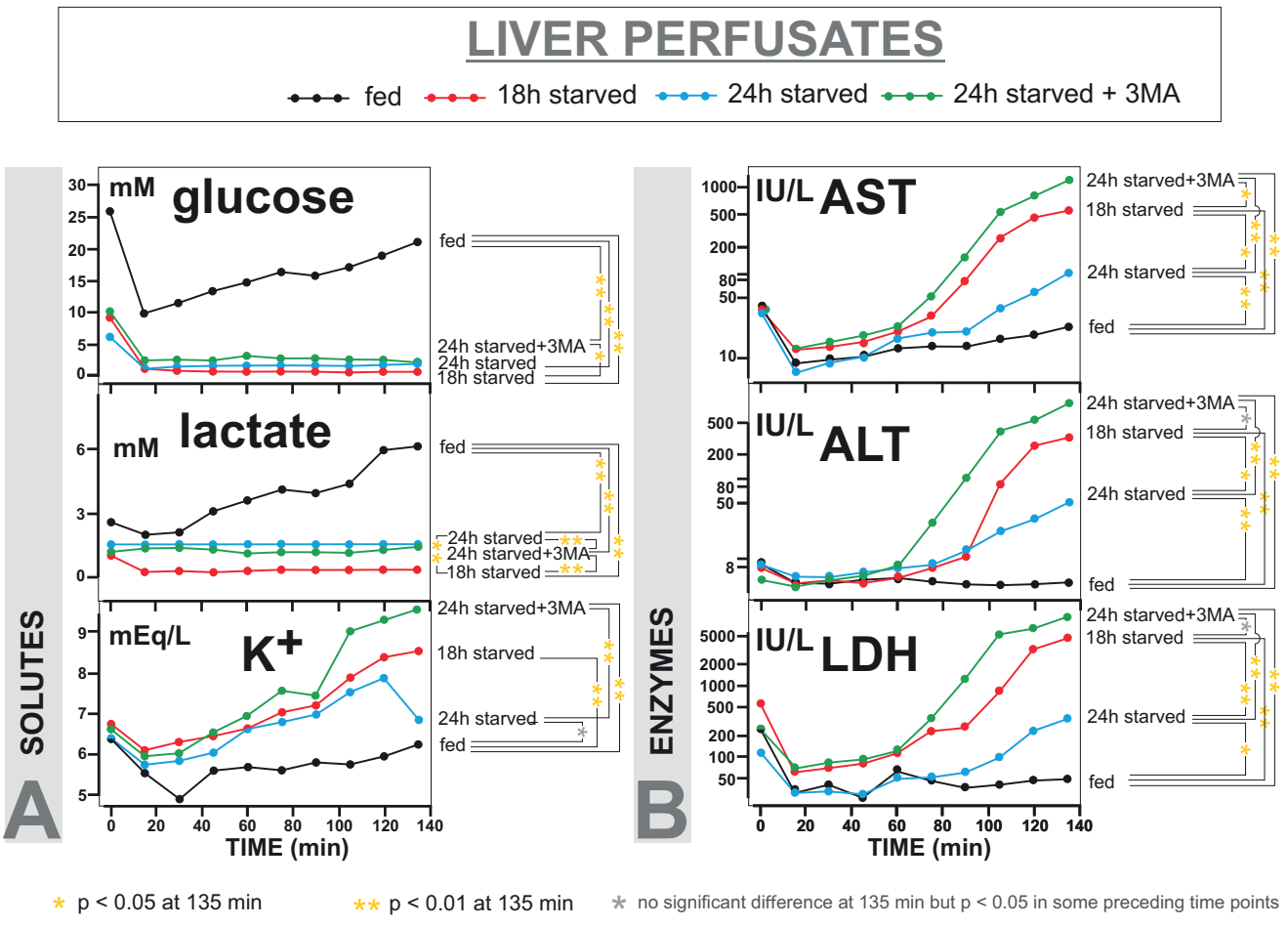

Fig. 1. Perfusate markers of ex vivo rat livers in the fed, 18-h fasted, 24-h fasted, and 24-h fasted + 3-MA groups. Perfusate concentrations of solutes (A) and enzyme activity (B) over time are expressed in normal and logarithmic scaling, respectively, with significant statistical differences between liver groups being given for values at the 135-min time point. 3-MA, 3-methyladenine; ALT, alanine transaminase; AST, aspartate transaminase; LDH, lactate dehydrogenase. Note that in contrast to all other ordinate scales, which start at 0, the ordinate scale of perfusate kalium starts at a 5 mEq/L value.

group ($P = 0.025$). Similar findings were obtained for ALT. At the end of perfusion, ALT activities in the 18-h fasted and 24-h fasted + 3-MA groups were not significantly different; these two groups having higher perfusate ALT levels than the 24-h fasted group. LDH values differed between the four groups after 45 min of perfusion. They turned out to be systematically lower in the fed group than in the 18-h ($P = 0.014$) and 24-h fasted + 3-MA ($P = 0.0001$) groups but not the 24-h fasted group. LDH values in the 18-h fasted and 24-h fasted + 3-MA groups were similar and significantly higher than in the 24-h fasted group.

Liver glycogen

At baseline, liver glycogen contents differed significantly between each group except between 24-h fasted and 24-h fasted + 3-MA (Figs. 2 and 3A). During perfusion, it significantly decreased in all groups. At 135 min, glycogen was still in higher in the fed group than in the 18-h fasted group ($P < 0.0001$), the latter group exhibiting glycogen content higher than in the two 24-h fasted groups ($P < 0.0001$). Glycogen content was lower in the 24-h fasted group than in 24-h fasted + 3-MA ($P = 0.014$).

Liver apoptosis

Photomicrographs of activated caspase-3 liver immunohistochemistry at 0 min (T_0) and 135 min (T_{135}) time points in fed, 18-h fasted, 24-h fasted, and 24-h fasted + 3-MA groups are shown in Figure 4. Apoptosis activity as measured by the percentage of activated caspase-3 was the same in all groups at baseline (Fig. 3B). At the end of perfusion, it differed between all groups except when comparing 24-h fasted + 3-MA with 18-h–fasted and 24-h–fasted groups (Fig. 3B).

Liver autophagy

LC3 II-to-actin ratio

The LC3 II-to-actin ratio was similar in all groups at baseline; however, after 135 min of perfusion it was found significantly higher in the 24-h fasted group than in the 18-h fasted and 24-h fasted + 3-MA groups, respectively. During perfusion, LC3 II-to-actin ratio values significantly increased in the 24-h–fasted group but remained unchanged in the other groups. The rise in autophagy was essentially lost under 3-MA (Fig. 3C). Figure 5 visualizes Western blotting bands of autophagy LC3 II and actin in livers after 135 min ex vivo perfusion in fed, 18-h fasted, 24-h fasted, and 24- h fasted + 3-MA groups.

p62-to-actin ratio

Figure 5 also visualizes Western blotting band of p62 (along with actin) in the various groups. As accounted for by boxplot representations appearing in Fig 3D, the p62-to-actin ratio differed significantly between groups at baseline, being higher in the fed group than in the 24-h fasted and 24-h fasted +3-MA groups and lower in the 24-h fasted than in the 18-h fasted and 24-h fasted + 3-MA groups. During perfusion, it decreased in the 18-h fasted and 24-h fasted groups but not in the fed and 24-h fasted + 3-MA groups (Fig. 3D). At 135 min, p62-to-actin ratio in the fed group was still higher than in the other groups. Interestingly, it was also higher in the 18-h fasted group than in 24-h fasted and 24-h fasted + 3-MA groups.

Discussion

In perfused ex vivo livers, protective mechanisms were previously suggested to require energy availability above a critical threshold [1]. In the present work, induction of autophagy was attested by an increase in LC3 II-to-actin ratio and a reduction in p62-to-actin ratio, which represent highly specific [1] and less specific markers of autophagy, respectively [10–12]. This was demonstrated on transition from 18-h to 24-h fasting and protected against fasting-driven exacerbation of liver vulnerability. In fasted groups, the link between protection against cytolysis and enhanced autophagy is stronger and more consistent than the link between protection and reduced apoptosis. After 135 min energy-free perfusion, cytolysis was significantly lower and autophagy higher in the 24-h fasted group compared with the 24-h fasted + 3-MA and 18-h fasted groups. Moreover, an inverse relationship between cytolysis and available energy sources (glycogen + autophagy) clearly emerged when comparing the four experimental groups. As illustrated by Figure 6, the inverse link between autophagy and cytolysis is adequately highlighted when

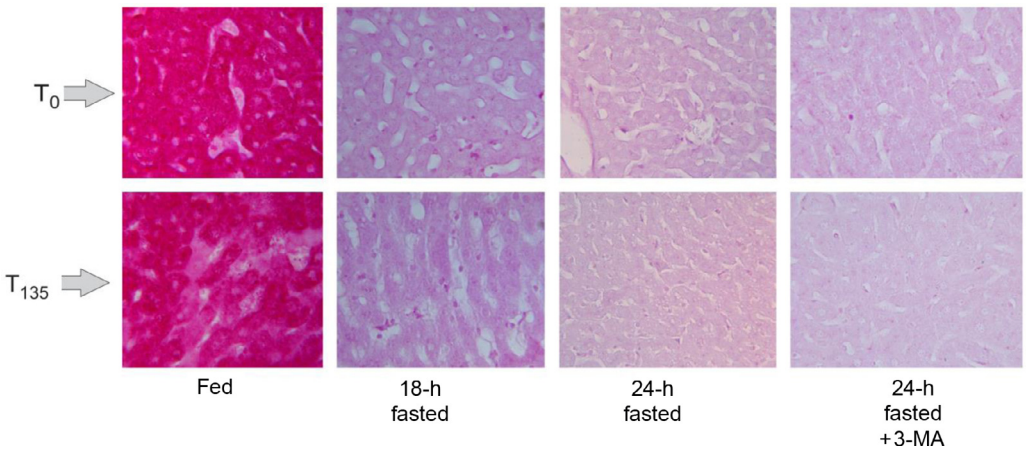

Fig. 2. Photomicrographs of PAS-stained liver slices at 0 min (T_0) and 135 min (T_{135}) time points in the fed, 18-h fasted, 24-h fasted, and 24-h fasted + 3-MA groups. The figure compares and illustrates PAS staining at the start and end of liver perfusions for one animal in each nutritional group. The abundance of glycogen is proportional to the red component of the PAS staining. As mentioned in the "Materials and Methods" section, PAS-stained slices were processed for determination of glycogen contents in hepatocytes at two time points (i.e., 0 and 135 min), using the Image J software (National Institutes of Health, Bethesda, MD, USA). The electronically determined staining intensity values determined on the whole experimental group are further accounted for by the boxplot representations appearing on Fig. 3A. PAS, periodic acid-Schiff.

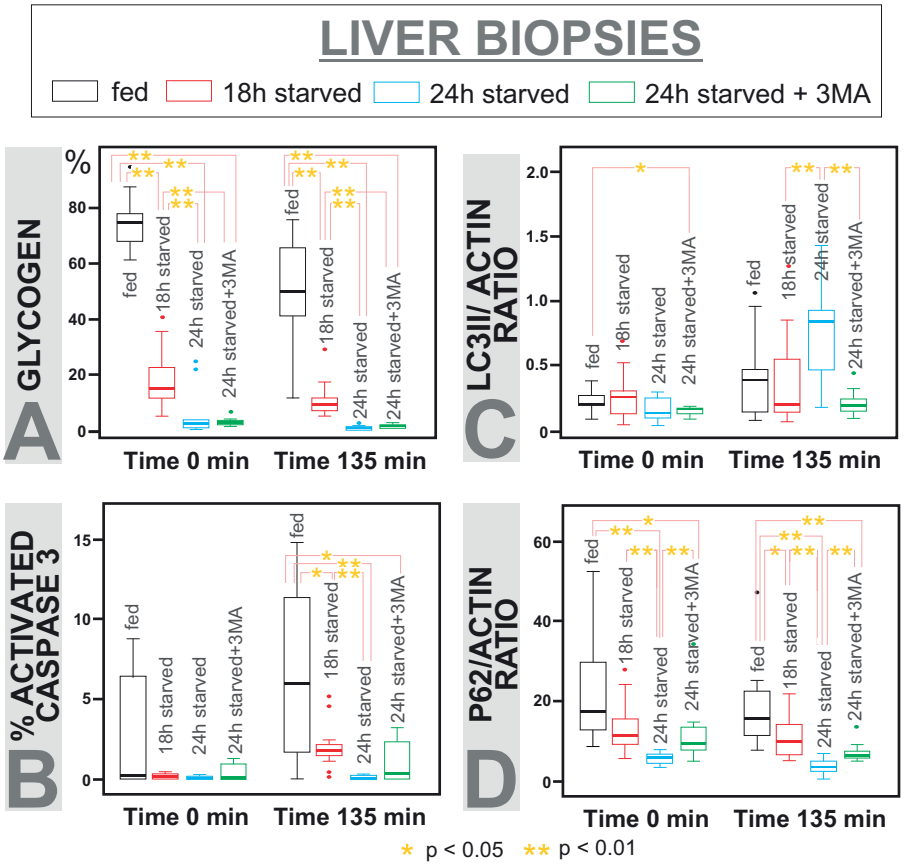

Fig. 3. Liver markers of ex vivo rat livers in the fed, 18-h fasted, 24-h fasted, and 24-h fasted + 3-MA groups. Box plots account for glycogen content (A), apoptosis activated caspase-3 (B), autophagy specific LC3 II-to-actin and (C) p62-to-actin (D) ratios. Significant statistical differences between liver groups are given for values at 0- and 135-min time points. 3-MA, 3-methyladenine.

considering autophagy as taking part, along with glycogen stores, in cellular energy mobilization capacities.

Because ex vivo liver is disconnected from circulating energetic substrates and infused with energy-free perfusion, glycogen represents a major energetic source. This latter is by far lower in fasted than in fed livers (Fig. 3A). Enhanced autophagy, known to provide cells with energetic substrates [15], would compensate for limited glycogen stores and protect against reduced energy stores. The higher the energy mobilization capacity, the lower the cytolysis (Fig. 6). Accordingly, inclusion of 3-MA in perfusion reduced

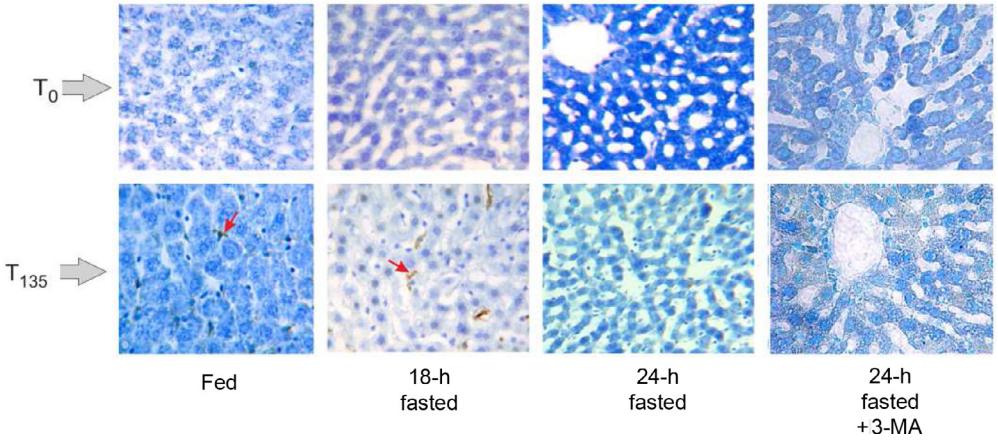

Fig. 4. Photomicrographs of activated caspase-3 liver immunohistochemistry at 0- (T_0) and 135-min (T_{135}) time points in the fed, 18-h fasted, 24-h fasted, and 24-h fasted + 3-MA groups. The figure compares and illustrates the immunolabeling at the start and end of liver perfusions for one animal in each nutritional group. The red arrow appearing on two photomicrographs, namely those at 135 min for both fed and 18-h fasted liver conditions, points to one of the immunolabeled cells seen on these liver photomicrographs. The immunolabeling is indicated by the visible brown coloration on photomicrographs (counterstaining being achieved by Toluidine blue). As mentioned in the "Materials and Methods" section, apoptosis counting was performed with the image J software using selection of cells immunolabeled for activated caspase-3, a determination of total and labeled cells by the image J cell counter, and subsequent calculation of labeled to total liver cell ratios. These counting values determined on the entire experimental group are accounted for by the boxplot representations appearing on Fig. 3B. 3-MA, 3-methyladenine.

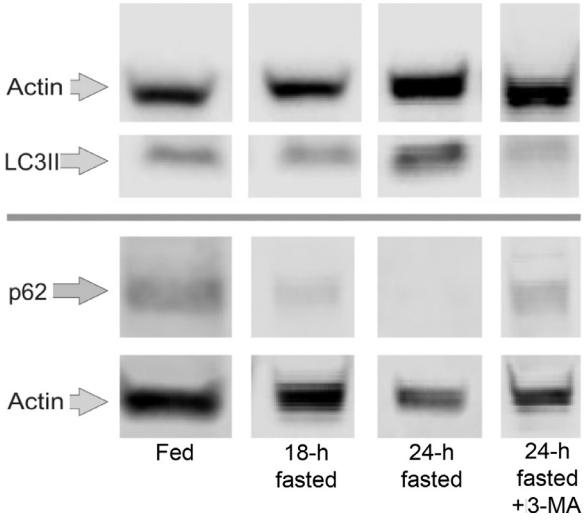

Fig. 5. Western blotting bands of autophagy LC3 II and p62 proteins and actin in livers after 135 min ex vivo perfusion in the fed, 18-h fasted, 24-h fasted, and 24-h fasted + 3-MA groups. The figure compares and illustrates that two separate runs were performed for assessing autophagy markers for one animal in each nutritional group: One run for LC3 II and a separate run for p62, each of these runs being also evaluated for actin content. The LC3 II and p62, along with actin associated with each of these runs, were quantified by Li-Cor software on selected areas. Data generated by the Li-Cor are highly reproducible and are not dependent on the operator and light exposure of blots. Li-Cor data were used for boxplot representations appearing in Figure 3C, D. 3-MA, 3-methyladenine.

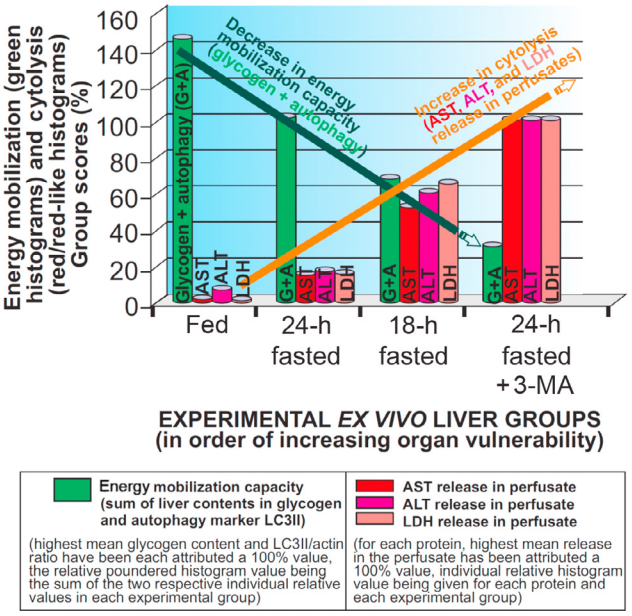

Fig. 6. Energy mobilization capacities versus cytolysis in ex vivo livers after exposure to a 135-min energy-free perfusion. Energy mobilization capacity in perfused ex vivo liver is essentially accounted for by the sum of glycogen stores and autophagic activity (assessed by LC3 II-to-actin ratio) in liver biopsies (Fig. 3A and C, respectively). Cytolysis is accounted for by releases of AST, ALT, and LDH in perfusates (Fig. 1B). Relative mean levels of energy mobilization capacity and proteins released in perfusates are expressed as percentage values, the 100% mean value referring to the highest level throughout experimental groups. Accordingly, a 100% mean value has been ascribed to glycogen from fed livers, to autophagy marker LC3 II-to-actin ratio from 24-h fasted livers, and to AST, ALT, and LDH releases from 24-h fasted + 3-MA livers. For protein releases in perfusate, the three calculated percentages are individually represented (red and red-like histograms). For energy mobilization capacity (green histograms), calculated percentages of glycogen and LC3 II/actin ratio have been summed (so percentage may exceed 100). The inverse relationship between energy mobilization capacity and cytolysis essentially accounts for protective roles of glycogen stores in fed conditions and of autophagic activity in starved conditions. 3-MA, 3-methyladenine; ALT, alanine transaminase; AST, aspartate transaminase; LDH, lactate dehydrogenase.

autophagic activity (Fig. 3C and D); it led to increased cytolysis (Fig. 1B) and hence loss of benefit given by 24-h versus 18-h fasting of rats, emphasizing that autophagy is highly protective.

A key determinant in interpreting changes in levels of released metabolites, in particular lactate, is disconnection of ex vivo livers from circulation, opposing ex vivo and in situ livers. For in situ liver, lactate release in circulation is primarily fueled from extrahepatic anaerobic glycolysis to contribute to Cori's cycle [16]. For perfused ex vivo livers, lactate release in perfusate, although virtually issued from anaerobic glycolysis by extrahepatocyte cells (Kupffer, vascular, duct cells, etc.) primarily accounts for, like glucose, hepatocyte gluconeogenesis. Indeed, owing to the absence of inclusion of glucose in perfusion and disconnection from circulation, the major glucose source from which lactate may derive is therefore hepatocyte gluconeogenesis, shading that, in return, lactate production depends on extrahepatocyte glycolysis rates and may aliment hepatocyte gluconeogenesis. Although perhaps paradoxical, higher glucose production in fed versus fasted conditions is indicative of higher glycogen stores [17]. Accordingly, lactate release is higher in fed versus fasted livers (Fig. 1A). Regarding fasted livers, higher lactate levels at 24 h versus 18 h of fasting might be explained by a higher background hepatocyte gluconeogenesis, perhaps as a result of a longer in vivo exposure to glucagon that interestingly, in contrast to the autophagy inhibitor insulin [18], promotes autophagy [19]. This higher lactate levels at 24 h versus 18 h of fasting is not affected by inclusion of 3-MA in perfusion, suggesting little or no compound effect on gluconeogenesis. Higher gluconeogenesis rates in the two 24-h versus the 18-h fasted groups might take place by consuming glycogen, explaining why glycogen contents were significantly lowered in former versus latter groups. The significant drop observed between hepatic glycogen contents of the 24-h fasted versus the 24-h fasted + 3-MAgroup is only very moderate and might be accounted for by glycogen autophagy, a special form of autophagy referred to as *glycophagy* [20] and most likely would be eliminated under autophagy inhibition by 3-MA.

Taken as a whole, present protective mechanisms are well accounted for in Figure 6. Owing to the present use of female animals, their potentiating by estrogen signaling cannot be ruled out. Since the pioneer work of de Duve, increased attention has been dedicated to the role of autophagy in programmed cell death and optional survival through well-designed experimental works [21–23]. In parallel and meanwhile, the clinical relevance of autophagy has also emerged in medical fields including surgery and oncology. Recently, the prognostic value of the autophagic marker LC3 was highlighted in two cohorts of patients undergoing liver resection as a surgical cure of hepatocellular carcinoma [24]. In this respect, liver regeneration after extended resections subsequent to neoadjuvant therapies represents a main issue where ischemic tolerance and remnant volume are of major interest. In light of the present work, these experimental and medical developments might also stress the interest in promoting cellular pathways involved in energy mobilization to trigger protective and survival effects.

References

[1] Papegay B, Stadler M, Nuyens V, Kruys V, Boogaerts JG, Vamecq J. Short fasting does not protect perfused ex vivo rat liver against ischemia-reperfusion. On the importance of a minimal cell energy charge. Nutrition 2017;35:21–7.
[2] Lemasters JJ, Nieminen AL, Qian T, Trost LC, Elmore SP, Nishimura Y, et al. The mitochondrial permeability transition in cell death: a common mechanism in necrosis, apoptosis and autophagy. Biochim Biophys Acta 1998;1366:177–96.

[3] Liu Y, Levine B. Autosis and autophagic cell death: the dark side of autophagy. Cell Death Differ 2015;22:367–76.
[4] Kiraz Y, Adan A, Kartal Yandim M, Baran Y. Major apoptotic mechanisms and genes involved in apoptosis. Tumour Biol 2016;37:8471–86.
[5] Green DR. Apoptotic pathways: ten minutes to dead. Cell 2005;121:671–4.
[6] He C, Klionsky DJ. Regulation mechanisms and signaling pathways of autophagy. Annu Rev Genet 2009;43:67–93.
[7] Stipanuk MH. Macroautophagy and its role in nutrient homeostasis. Nutr Rev 2009;67:677–89.
[8] Stadler M, Nuyens V, Seidel L, Albert A, Boogaerts JG. Effect of nutritional status on oxidative stress in an ex vivo perfused rat liver. Anesthesiology 2005;103:978–86.
[9] Hengartner MO. The biochemistry of apoptosis. Nature 2000;407:770–6.
[10] Barth S, Glick D, Macleod KF. Autophagy: assays and artifacts. J Pathol 2010;221:117–24.
[11] Klionsky DJ, Abdelmohsen K, Abe A, Abedin MJ, Abeliovich H, Acevedo Arozena A, et al. Guidelines for the use and interpretation of assays for monitoring autophagy. Third edition. Autophagy 2016;12:1–222.
[12] Mizushima N, Yoshimori T. How to interpret LC3 immunoblotting. Autophagy 2007;3:542–5.
[13] Seglen PO, Gordon PB. 3-methyladenine: specific inhibitor of autophagic/lysosomal protein degradation in isolated rat hepatocytes. Proc Natl Acad Sci USA 1982;79:1889–92.
[14] Stadler M, Nuyens V, Boogaerts JG. Intralipid minimizes hepatocytes injury after anoxia-reoxygenation in an ex vivo rat liver model. Nutrition 2007;23:53–61.
[15] Singh R, Cuervo AM. Autophagy in the cellular energetic balance. Cell Metab 2011;13:495–504.
[16] Cori CF. The glucose-lactic acid cycle and gluconeogenesis. Curr Top Cell Regul 1981;18:377–87.
[17] Hems DA, Whitton PD. Control of hepatic glycogenolysis. Physiol Rev 1980;60:1–50.
[18] Paula-Gomes S, Gonçalves DAP, Baviera AM, Zanon NM, Navegantes LCC, Kettelhut IC. Insulin suppresses atrophy- and autophagy-related genes in heart tissue and cardiomyocytes through AKT/FOXO signaling. Horm Metab Res 2013;45:849–55.
[19] Schworer CM, Mortimore GE. Glucagon-induced autophagy and proteolysis in rat liver: Mediation by selective deprivation of intracellular amino acids. Proc Natl Acad Sci U S A 1979;76:3169–73.
[20] Jiang S, Wells CD, Roach PJ. Starch-binding domain-containing protein 1 (Stbd1) and glycogen metabolism: identification of the Atg8 family interacting motif (AIM) in Stbd1 required for interaction with GABARAPL1. Biochem Biophys Res Commun 2011;413:420–5.
[21] De Duve C, Wattiaux R. Functions of lysosomes. Annu Rev Physiol 1966;28:435–92.
[22] Komatsu M, Waguri S, Ueno T, Iwata J, Murata S, Tanida I, et al. Impairment of starvation-induced and constitutive autophagy in Atg7 to deficient mice. J Cell Biol 2005;169:425–34.
[23] Mortimore GE, Pösö AR. Intracellular protein catabolism and its control during nutrient deprivation and supply. Annu Rev Nutr 1987;7:539–64.
[24] Lin CW, Lin CC, Lee PH, Lo GH, Hsieh PM, Koh KW, et al. The autophagy marker LC3 strongly predicts immediate mortality after surgical resection for hepatocellular carcinoma. Oncotarget 2017;8:91902–13.